UCSF

Title

High-Resolution 3-T Endorectal Prostate MRI: A Multireader Study of Radiologist Preference and Perceived Interpretive Quality of 2D and 3D T2-Weighted Fast Spin-Echo MR Images.

Authors

Westphalen, Antonio C
Noworolski, Susan M
Harisinghani, Mukesh
et al.

High-Resolution 3-T Endorectal Prostate MRI: A Multireader Study of Radiologist Preference and Perceived Interpretive Quality of 2D and 3D T2-Weighted Fast Spin-Echo MR Images

Antonio C. Westphalen[1], **Susan M. Noworolski**[1], **Mukesh Harisinghani**[2], **Kartik S. Jhaveri**[3], **Steve S. Raman**[4], **Andrew B. Rosenkrantz**[5], **Zhen J. Wang**[1], **Ronald J. Zagoria**[1], and **John Kurhanewicz**[1]

[1]Department of Radiology and Biomedical Imaging, University of California, San Francisco, 505 Parnassus Ave, M-372, Box 0628, San Francisco, CA 94143

[2]Department of Radiology, Massachusetts General Hospital, Harvard Medical School, Boston, MA

[3]Joint Department of Medical Imaging, University Health Network, Mount Sinai and Women's College Hospital, University of Toronto, Toronto, ON, Canada

[4]Department of Radiology, David Geffen School of Medicine at University of California, Los Angeles, Los Angeles, CA

[5]Department of Radiology, New York University, Langone Medical Center, New York, NY

Abstract

OBJECTIVE—The goal of this study was to compare the perceived quality of 3-T axial T2-weighted high-resolution 2D and high-resolution 3D fast spin-echo (FSE) endorectal MR images of the prostate.

MATERIALS AND METHODS—Six radiologists independently reviewed paired 3-T axial T2-weighted high-resolution 2D and 3D FSE endorectal MR images of the prostates of 85 men in two sessions. In the first session ($n = 85$), each reader selected his or her preferred images; in the second session ($n = 28$), they determined their confidence in tumor identification and compared the depiction of the prostatic anatomy, tumor conspicuity, and subjective intrinsic image quality of images. A meta-analysis using a random-effects model, logistic regression, and the paired Wilcoxon rank-sum test were used for statistical analyses.

RESULTS—Three readers preferred the 2D acquisition (67–89%), and the other three preferred the 3D images (70–80%). The option for one of the techniques was not associated with any of the predictor variables. The 2D FSE images were significantly sharper than 3D FSE ($p < 0.001$) and significantly more likely to exhibit other (nonmotion) artifacts ($p = 0.002$). No other statistically significant differences were found.

CONCLUSION—Our results suggest that there are strong individual preferences for the 2D or 3D FSE MR images, but there was a wide variability among radiologists. There were differences in image quality (image sharpness and presence of artifacts not related to motion) but not in the sequences' ability to delineate the glandular anatomy and depict a cancerous tumor.

Keywords

artifact; MRI; prostate cancer; quality; T2-weighted MRI

A multiparametric prostate MRI examination is a relatively long procedure, often lasting 45–60 minutes, depending on the sequences acquired. Approximately 20–25% of this time is used for the acquisition of high-resolution T2-weighted 2D fast spin-echo (FSE) MR images in the three orthogonal planes. Yet, most radiologists base their anatomic assessment of the prostate on axial images alone and use the other planes to localize abnormalities into the craniocaudal axis, estimate the gland's volume, and confirm findings seen in the axial plane.

Each of these 2D sequences is typically acquired at a 3-mm slice thickness. To acquire a 3D T2-weighted sequence of this volume with submillimeter resolution in each plane using historically available parameters would be prohibitively long. Novel 3D FSE sequences that incorporate various acceleration schemes allow the acquisition of volume data that can be reconstructed into any plane in much less time [1, 2]. These 3D sequences may allow improved delineation of anatomy and accurate detection of smaller tumors owing to reduced partial volume averaging effect.

Importantly, some trade-offs are inevitable so that these 3D volumes can be generated in a reasonable scan time. For example, a shorter TR can greatly shorten the sequence scan time at the cost of incorporating more T1-weighting and change in image contrast. Also, even subtle motion during the 3D FSE acquisitions will lead to blurring and loss of resolution that affects the entire volume.

Although 3D sequences have been tested in the setting of neuroradiology and musculoskeletal imaging [3, 4], little data exist for prostate MRI [5–7]. Furthermore, to our knowledge all data to date have been derived from 1.5-T magnets, and the current recommendation is that men with prostate cancer, whenever possible, undergo imaging with 3-T scanners [8]. Only two of these studies made a direct comparison between 3D and 2D FSE MR images [5, 6], and one of these did not use an endorectal coil [6]. Although many radiologists consider the endorectal coil to be an optional tool for the assessment of prostate cancer [9], it leads to higher signal-to-noise ratio, which could improve anatomic assessment and tumor characterization. However, the use of an endorectal coil could also increase artifacts because of its nonuniform reception profile [10]. The goal of this study was therefore to compare the perceived quality of 3-T axial T2-weighted high-resolution 2D and high-resolution 3D FSE endorectal MR images of the prostate.

Materials and Methods

The institutional review board of the center where imaging was performed approved this retrospective HIPAA-compliant study. At the time of imaging, all patients signed a consent form allowing use of their imaging data for future studies.

Patient Population

This study included 85 consecutive men (median age, 65 years; age range, 46–83 years) who underwent prostate MRI at the University of California, San Francisco, between April 14 and June 17, 2014. Most of these men (74/85 [87%]) had biopsy-proven prostate cancer, whereas the remaining patients had suspected disease on the basis of elevated prostate-specific antigen (PSA) but no prior biopsy. The Gleason scores of men with known cancer were 3 + 3 (48/74 [65%]), 3 + 4 (17/74 [23%]), 4 + 3 (7/74 [9%]), and 4 + 4 (2/74 [3%]). The mean (± SD) PSA level was 6.8 ± 4.8 ng/mL (range, 0.52–30.6 ng/mL). Most men with known prostate cancer were being managed with active surveillance (56/74 [76%]), but 18 had received prior treatment as follows: permanent prostatic implant brachytherapy (10/74 [14%]), external beam radiation therapy (4/74 [5%]), focal cryoablation (2/74 [3%]), and androgen deprivation therapy (2/74, 3%).

Imaging Acquisition

All scans were done on a 3-T scanner (Discovery MR750, GE Healthcare) using a body coil for excitation and an inflatable endorectal coil (E-Coil, Medrad) filled with perfluorocarbon in conjunction with a pelvic phased-array coil for reception. All MR images were postprocessed to compensate for the reception profile of the endorectal and pelvic phased-array coils [10].

Our protocol included two T2-weighted MRI acquisitions, designated A and B. The first of these sequences consisted of thin-section high-spatial-resolution axial, sagittal, and coronal T2-weighted 2D FSE MR images of the prostate and seminal vesicles obtained using the following parameters: FOV, 18 cm; TR/effective TE, 5600–7400/99–114; echo-train length, 16; section thickness, 3 mm; no intersection gap; acquisition matrix, 384 × 384 (512 × 512 reconstruction); frequency direction, anteroposterior, flip angle, 111°; and 1 signal excitation. The final, reconstructed voxel size was $0.35 \times 0.35 \times 3$ mm. The second of these sequences consisted of T2-weighted 3D FSE MR images of the prostate and seminal vesicles obtained with the cube sequence [11] using the following parameters: FOV, 18 cm; TR/TE, 1800/117; echo-train length, 90; section thickness, 1.6 mm; acquisition matrix, 256 × 256 (512 × 512 interpolated matrix in-plane and twofold along the craniocaudal axis); effective thickness, 0.8 mm; frequency direction, anteroposterior; flip angle, 90°; 2 signal excitations; and receiver bandwidth, 90.91 kHz). Parallel imaging (generalized autocalibrating partially parallel acquisition in the phase direction) was used, and the final, reconstructed voxel size was $0.35 \times 0.35 \times 0.8$ mm.

The parameters of the 3D sequence—for example, TR and echo-train length—were chosen to result in the same in-plane resolution as the 2D sequence with a similar acquisition time of less than 5 minutes.

T1-weighted MR images, DW images, dynamic contrast-enhanced MR images, and MR spectroscopic images, although also acquired, were not reviewed by the readers in this study. Sagittal and coronal T2-weighted 2D FSE MR images were also not included in this study.

Image Review

Six radiologists with 5–20 years of dedicated experience in prostate MRI independently reviewed de-identified axial T2-weighted MR images of 85 consecutive patients. Each reader was given an unmarked set of 100 computerized slides (PowerPoint for Mac 2011 [version 14.4.2], Microsoft) to review, 15 of which were duplicates; radiologists were not aware of these duplicated slides. Each slide contained a pair of T2-weighted MR images, one acquired using 3D FSE and one acquired using 2D FSE. Both images corresponded to the same location in the gland, and the window width and level were set to display the images similarly. On half of the slides, the 3D FSE image was located on the right side of the slide, and on the other half, on the left side. Eight of the duplicated images were presented in the reverse order of their counterparts (right/left and left/right). One radiologist with 10 years of dedicated experience in prostate MRI who did not participate in the review of images randomly selected from each study the slices used for the comparison. In 42 cases, this choice was made first using 3D FSE images; for the remaining 43 cases, the selecting radiologist started with the 2D FSE acquisition. The order in which the 100 slides were presented to readers was randomly determined using a free software plug-in (Random Slides, OfficeOne). Figure 1 shows one of the slides presented to radiologists. Readers were asked to identify their preferred image.

Three weeks after the last radiologist evaluated the 100-slide presentation, an additional set of axial T2-weighted 2D and 3D FSE MR images were submitted to each reader for independent review. In this collection, we included images only of patients with biopsy-proven prostate cancer containing Gleason 4 pattern in the corresponding location (sextant) and for whom at least two of three functional MR sequences (DWI, dynamic contrast-enhanced MRI, and MR spectroscopy) yielded positive findings concordant with the findings based on the T2-weighted MR images. A positive finding on DWI was defined as high signal intensity on the DW images and low signal intensity on the apparent diffusion coefficient map. A positive finding on dynamic contrast-enhanced MRI was defined as asymmetric enhancement showing a steep wash-in slope and fast washout. A positive finding on MR spectroscopy was defined as three or more consecutive voxels showing a choline peak at least one to two times higher than the citrate peak. There were 14 studies that met these criteria.

A single radiologist selected the image from each study that best depicted the tumor. In half of the cases, this selection was done by using the 2D FSE acquisition and then identifying the corresponding image on the 3D FSE sequence; the process was the opposite for the remaining cases. A total of 28 paired images were selected. The final presentation had two parts, the first of which consisted of 28 slides, each with a single T2-weighted 2D FSE or 3D FSE MR image. These slides were presented in a random order, and readers were asked to score their confidence in identifying a tumor from 1 (not confident) to 5 (very confident). In

the second part, the slides showed the same images but paired (2D/3D or 3D/2D). At this time, the readers were informed that all images depicted a visible tumor. Readers were again asked not only to select which of the two images was preferred but also to justify their choice using a simple survey. The survey had questions related to the prostatic anatomy (delineation of the zonal anatomy and prostatic capsule), tumor conspicuity (contrast between tumor and normal glandular tissue), and image quality (motion artifact, other nonmotion artifacts, distortion, and image sharpness). Other nonmotion artifacts refer to any other artifact that was not attributable to coil or patient motion. Each of these items was rated using a 3-point scale (for prostatic anatomy and tumor conspicuity: 1, poor; 2, good; 3, excellent; for image quality [except image sharpness]: 1, marked; 2, some; 3, none). All images were imported directly into PowerPoint as TIFFs, using a proprietary teaching file system.

Statistical Analyses

Descriptive statistics and the corresponding measures of dispersion were used to summarize the population characteristics. Chi-square testing was used to analyze the data from duplicate slides. A statistically significant result indicates that the radiologist chose the same technique in most instances; that is, the option for the same technique each time the slide was presented was beyond the expected chance distribution.

There are two sources of variation in this study: the slides presented to the radiologists and the individual radiologists who rated the slides. To clearly separate these two sources of variation, we used a two-level analysis—first summarizing the data for each radiologist, then summarizing the data across radiologists to account for the uncertainty for each radiologist. This was accomplished by means of a meta-analysis using a random-effects model. A formal analysis of heterogeneity was also done. The presence of heterogeneity, characterized by a statistically significant result, suggests that there were differences in the readers' scores, which may have been driven by outliers. When scores are symmetrically distributed, heterogeneity suggests a large dispersion.

We used logistic regression to determine if prior treatment (categoric variable), number of years of experience (ordinal variable), and radiologist (categoric variable) were predictors of the choice for 2D or 3D images. We tested each predictor using a univariate model, and irrespective of the result of these models, all variables were also included in a multivariate model. Nonetheless, because six readers evaluated all the images, we also performed a multivariate mixed effect logistic regression to take into account the effect of multiple readers.

For the second part of our study—the assessment of confidence in tumor identification, tumor conspicuity, anatomic delineation (zonal anatomy and capsular delineation), and image quality (motion artifact, other artifacts, distortion, and image sharpness) in patients with visible tumor—we performed two analyses. First, we compared the overall scores of the two sequences using the paired Wilcoxon rank-sum test. Next, we performed the meta-analyses as already described.

Statistical calculations were performed using Stata (version 13.1, StataCorp). All tests were two tailed, and a 5% level of confidence was considered statistically significant.

Results

Duplicate Slides

The intrareader agreement, defined as the frequency with which a reader preferred the same T2-weighted MR sequence (2D vs 3D) when presented with duplicate slides, ranged from 60% to 100% (Table 1). Although all radiologists opted for the same technique in most instances when a duplicate slide was presented, two readers showed a weaker preference for the choices made ($p = 0.14$ and 0.40).

Preferred Imaging Sequence

Figure 2 and Table 2 show that each reader had a strong individual preference for a given T2-weighted MR sequence, favoring one of the two techniques in at least approximately 70% of cases, and that the choices were evenly distributed between the two sequence options. Three readers strongly preferred the 2D FSE acquisition (67–89%), and the other three readers strongly preferred the 3D FSE acquisition (70–80%).

Assessment of Predictors of Preferred Sequence

The option for one of the T2-weighted MRI techniques was not associated with prior treatment or readers' years of experience on univariate or multivariate logistic regressions. Given the lack of a clustering effect related to the multiple readers, we used logistic regression without a mixed effect model (Table 3).

Confidence in Tumor Identification

There was no significant difference in confidence in tumor identification when comparing 2D and 3D FSE MR images for any reader ($p = 0.16$–1.00) (Fig. 3 and Table 4).

Tumor Conspicuity, Anatomic Delineation, and Image Quality

As seen with the entire sample, individual authors showed a preference for one or the other sequence in the subset analyses that was almost equally distributed (Fig. 4). The pooled estimate suggests an option for the 3D image is expected approximately 40% of the time (95% CI, 17–64%).

There was no difference in delineation of the zonal anatomy ($p = 0.19$), prostatic capsule ($p = 0.14$), and tumor conspicuity ($p = 0.89$) when comparing 2D and 3D FSE MR images. Similarly, no difference was found when assessing motion artifact ($p = 0.48$) and distortion ($p = 0.41$). The 2D FSE images were not only significantly sharper than 3D FSE ($p < 0.001$) but also significantly more likely to exhibit other (nonmotion) artifacts ($p = 0.002$). These results are summarized in Table 5.

Discussion

Although radiologists individually tended to strongly prefer either 2D or 3D FSE T2-weighted MR images, there was an equal split regarding the preferred sequence among the six radiologists in this study. Furthermore, the two sequences were not different in their ability to delineate the prostatic anatomy (zonal anatomy and prostatic capsule) and to depict a cancerous tumor, as shown by the results of the comparison of confidence in tumor identification and tumor conspicuity. In addition, no differences were noted in regards to image distortion and motion artifact. The 2D FSE images were significantly sharper than the 3D FSE images, but they were also more likely to exhibit other (non-motion) artifacts.

Because artifacts could affect these images differently, as indeed shown by our results, we tested to determine whether prior treatments would influence the option of readers. Images of patients treated with permanent prostatic implant brachytherapy, in particular, are prone to susceptibility artifact owing to the presence of the gold seeds. Our results, however, did not suggest that chosen treatment influenced the choices made by the radiologists. Another factor that could have influenced the choice of sequence is the number of years of experience of each reader. It is conceivable that more experienced readers would more likely prefer the 2D images over the 3D images, owing to their familiarity with that sequence. Variability in the preference for the 2D or 3D FSE acquisition among the six radiologists and lack of association with treatment and reader experience, however, suggests that individual preferences are based on other unmeasured subjective reasons.

In 2009, Panebianco et al. [5] reported the results of a study of 53 men who underwent 1.5-T endorectal prostate MRI using 2D and 3D T2-weighted turbo spin-echo (TSE) sequences (synonymous with FSE) to assess changes to the neurovascular bundles after nerve-sparing radical retropubic prostatectomy and to correlate these findings with post-treatment erectile function. According to their results, the imaging findings on the 3D sequences better correlated with the International Index Erectile Function Five-Item (IIEF-5) score. The results of the study by Panebianco et al. suggest that 3D TSE MR images better depict the anatomy of the neurovascular bundle, likely owing to the high-resolution isotropic acquisition. In our study, we did not include any patient who had undergone nerve-sparing surgery, nor did we specifically analyze the neurovascular bundles. Nonetheless, we did not find any difference between the two acquisitions in the anatomic assessments of the zonal anatomy and prostatic capsule on images acquired using a 3-T magnet. Further research is necessary to confirm or refute the results published by Panebianco et al.

A year later, Rosenkrantz et al. [6] published a study in which 1.5-T 3D T2-weighted TSE MR images were compared with multi-planar 2D T2-weighted TSE MR images, both acquired without an endorectal coil. In their study, 2D TSE MR images had higher signal-to-noise ratio, and 3D TSE MR images had better tumor conspicuity. Nonetheless, in spite of these differences, there were no significant differences in the accuracy of the two sequences for the diagnosis or staging of prostate cancer or in the subjective assessment of image quality. Our results are similar to those reported by Rosenkrantz et al. and suggest that either sequence is adequate for the assessment of patients with prostate cancer, irrespective of the use of an endorectal coil, specific vendor platform, and, perhaps, magnet strength.

Cornud et al. [7] found that the combination of direct and indirect signs of extracapsular extension on 1.5-T endorectal 3D TSE T2-weighted MRI have very good accuracy for its detection. Perhaps more significant, imaging had a very high negative predictive value, greater than 90%. Unfortunately, as Cornud et al. acknowledged, they did not perform a comparison with 2D acquisition, and the relative staging performance of 2D and 3D TSE T2-weighted images in this cohort remains unknown.

Because the acquisition parameters of our 2D sequence varied slightly from patient to patient, the time to obtain high-resolution 2D FSE images in three planes ranged from approximately 8 to 9 minutes. The acquisition time of our 3D FSE sequence, however, averages 4 minutes 30 seconds, which represents a 44% reduction in scanning time. Of course, this time saving can be realized only if 3D images can truly replace 2D ones, rather than serving as an additional sequence. In this study, axial 2D and 3D FSE images were of similar image quality, anatomic detail, and tumor conspicuity—results that support such a decision. Although some radiologists may strongly prefer the 2D acquisition, there was no consistency in the choices made, which seemed to be idiosyncratic. Nonetheless, additional studies comparing multiplanar images acquired with the two sequences may be necessary to corroborate our results.

The uses of 3D images will likely expand beyond diagnosis and staging of prostate cancer. For example, these images may be optimal for ultrasound-MRI fusion technologies used to guide biopsies and focal therapy. Such methods require not only accurate identification of tumors but also precise delineation of the gland to minimize misregistration at the time of fusion. Although 2D images are routinely used for this purpose in many institutions, it is conceivable that the outlining of the prostatic volume is improved by the use of a greater number of submillimeter images. These last claims, however, are hypothetical and should be the focus of further research.

Our study has limitations. Readers reviewed only a single 2D and a single 3D FSE MR image of each case, rather than the entire sequence. This was done to ensure evaluation of identical images by all six readers from multiple institutions. It is conceivable, however, that a single image is not representative of the entire study. However, to minimize this problem, we randomly selected the image, and it is expected that nonrepresentative images would be equally distributed in the two groups. Furthermore, the optimal window width and level is subjective. In this study, readers were not able to change these parameters, and this may have had an effect on the results. In an attempt to mitigate this factor, we included six readers in our study. We did not compare signal-to-noise measurements between the two sequences given our focus on radiologists' preference as applicable to everyday practice. Also, we did not have prostatectomy specimens in the 14 cases used in our secondary analyses. Although prostatectomy specimens were not available for the secondary analysis, our goal was to compare tumor conspicuity, not diagnostic accuracy. All lesions were histologically confirmed at biopsy as having primary Gleason 4 pattern and had corresponding abnormalities on multiple other MR sequences. That there were multiple positive MR sequences implies a high positive predictive value for confirming that the identified abnormality will correspond with a tumor at histopathology [12]. In addition, our sample size was small, limiting our statistical power. Finally, only axial images were

studied, and we cannot assume that a comparison of coronal and sagittal reconstructions from 3D acquisitions and 2D sagittal and coronal images would yield similar results. It is possible that one sequence would be consistently considered better if these other planes had been also investigated.

In conclusion, our results suggest that there are strong individual preferences for the 2D or 3D FSE MR images, but there was wide variability in preference among radiologists. There were differences in image quality (image sharpness and presence of artifacts not related to motion) but not in the sequences' ability to delineate the glandular anatomy and depict a cancerous tumor. Nonetheless, 3D FSE images might be a better option when time saving is crucial. Additionally, the use of 3D acquisitions may allow the expansion of other applications such as ultrasound-MRI fusion to guide biopsies and focal therapy; these last claims are hypothetical and should be the focus of further research.

Acknowledgments

References

1. Lichy MP, Wietek BM, Mugler JP 3rd, et al. Magnetic resonance imaging of the body trunk using a single-slab, 3-dimensional, T2-weighted turbo-spin-echo sequence with high sampling efficiency (SPACE) for high spatial resolution imaging: initial clinical experiences. Invest Radiol. 2005; 40:754–760. [PubMed: 16304477]

2. Busse RF, Brau AC, Vu A, et al. Effects of refocusing flip angle modulation and view ordering in 3D fast spin echo. Magn Reson Med. 2008; 60:640–649. [PubMed: 18727082]

3. Stevens KJ, Busse RF, Han E, et al. Ankle: isotropic MR imaging with 3D-FSE-cube—initial experience in healthy volunteers. Radiology. 2008; 249:1026–1033. [PubMed: 19011194]

4. Tagliafico A, Succio G, Neumaier CE, et al. Brachial plexus assessment with three-dimensional isotropic resolution fast spin echo MRI: comparison with conventional MRI at 3. 0 T. Br J Radiol. 2012; 85:e110–e116. [PubMed: 21343321]

5. Panebianco V, Sciarra A, Osimani M, et al. 2D and 3D T2-weighted MR sequences for the assessment of neurovascular bundle changes after nerve-sparing radical retropubic prostatectomy with erectile function correlation. Eur Radiol. 2009; 19:220–229. [PubMed: 18651150]

6. Rosenkrantz AB, Neil J, Kong X, et al. Prostate cancer: comparison of 3D T2-weighted with conventional 2D T2-weighted imaging for image quality and tumor detection. AJR. 2010; 194:446–452. [PubMed: 20093608]

7. Cornud F, Rouanne M, Beuvon F, et al. Endorectal 3D T2-weighted 1 mm-slice thickness MRI for prostate cancer staging at 1.5 tesla: should we reconsider the indirects signs of extracapsular extension according to the D'Amico tumor risk criteria? Eur J Radiol. 2012; 81:e591–e597. [PubMed: 21871750]

8. Barentsz JO, Richenberg J, Clements R, et al. ESUR prostate MR guidelines 2012. Eur Radiol. 2012; 22:746–757. [PubMed: 22322308]

9. American College of Radiology. MR Prostate Imaging Reporting and Data System version 2.0. Reston, VA: American College of Radiology; 2014.

10. Noworolski SM, Reed GD, Kurhanewicz J, Vigneron DB. Post-processing correction of the endorectal coil reception effects in MR spectroscopic imaging of the prostate. J Magn Reson Imaging. 2014; 32:654–662. [PubMed: 20815064]

11. Mugler JP 3rd. Optimized three-dimensional fast-spin-echo MRI. J Magn Reson Imaging. 2014; 39:745–767. [PubMed: 24399498]

12. Pinto PA, Chung PH, Rastinehad AR, et al. Magnetic resonance imaging/ultrasound fusion guided prostate biopsy improves cancer detection following transrectal ultrasound biopsy and correlates
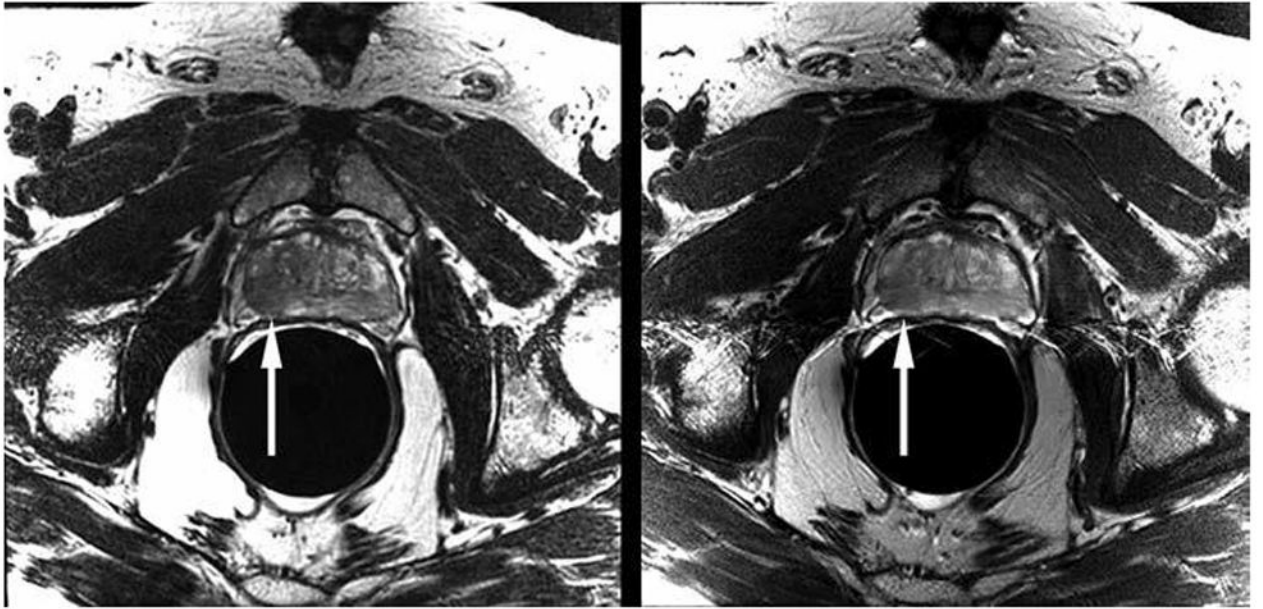
with multiparametric magnetic resonance imaging. J Urol. 2011; 186:1281–1285. [PubMed: 21849184]

Fig. 1.
Example computerized slide shown to readers (PowerPoint for Mac 2011 [version 14.4.2], Microsoft) comprises axial T2-weighted 3D fast spin-echo (FSE) MR image (*left*) and corresponding 2D FSE image (*right*). This 68-year-old man had biopsy-proven prostate cancer in peripheral zone of right mid gland. Tumor is visible on both images as focal area of decreased signal intensity (*arrows* [not present on slides reviewed by readers]).
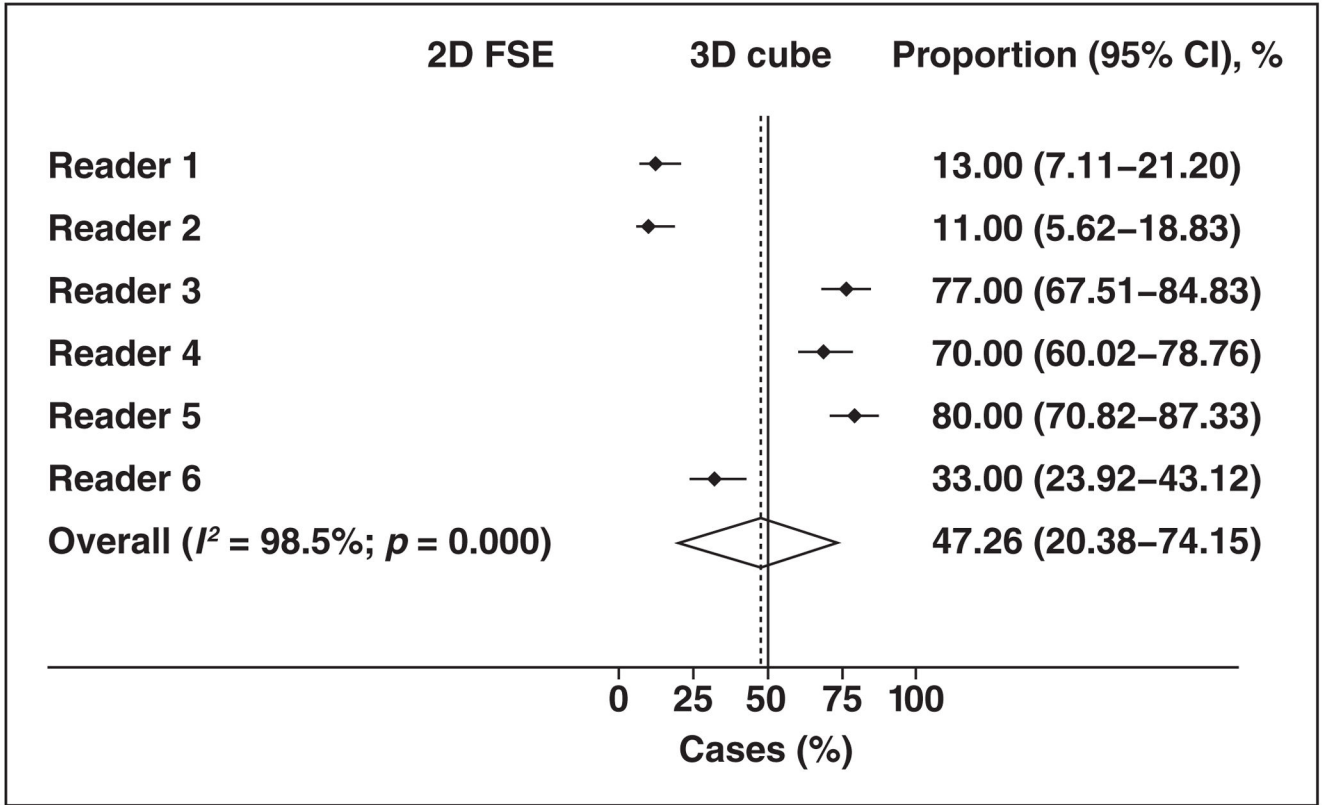
Fig. 2.
Forest plot shows individual preferences for given T2-weighted MR sequence for entire sample. Summary estimate (*diamond*) indicates that there was almost equal distribution of such preferences between two options. Dashed line denotes summary measure. FSE = fast spin-echo.
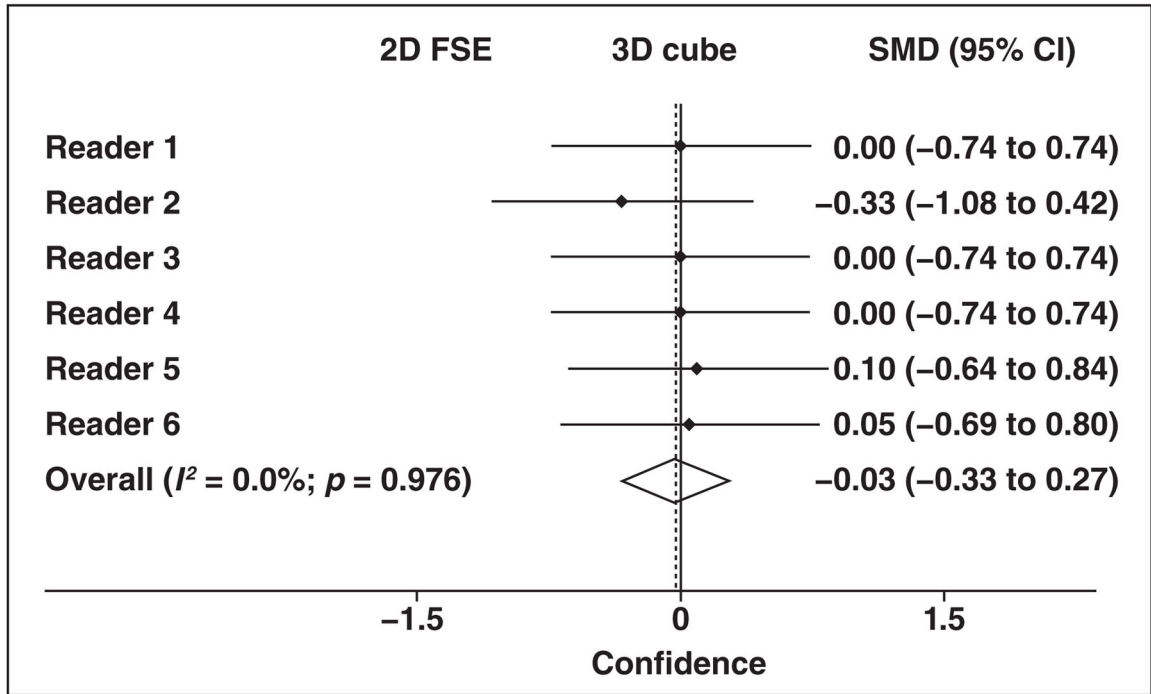
Fig. 3.
Forest plot shows readers' confidence in tumor identification. Summary estimate (*diamond*) indicates that there was no overall difference in confidence of tumor identification based on T2-weighted MR sequence. Reader 2 had tendency to be more confident after assessing 2D fast spin-echo (FSE) sequence, but 95% CI intersects 0 point. Dashed line denotes summary measure. SMD = standardized mean difference.
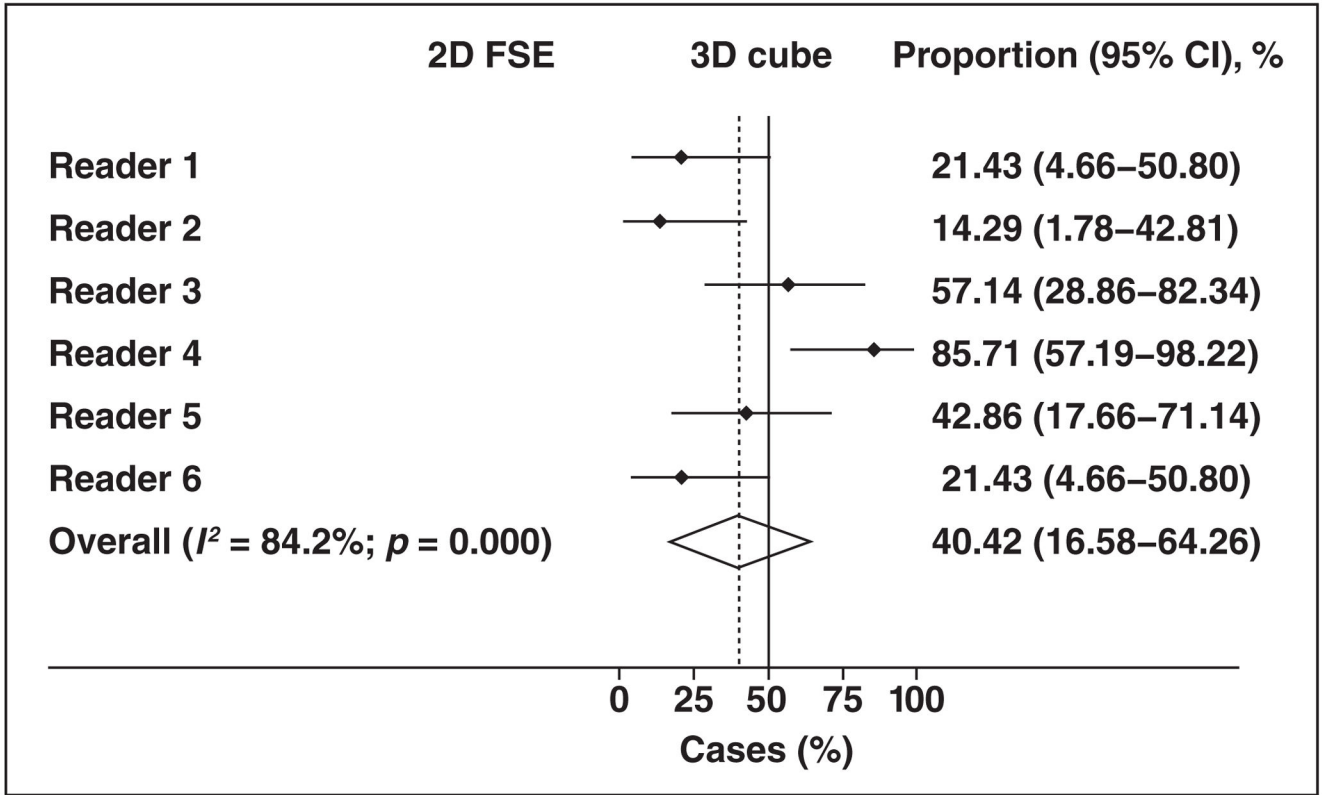
Fig. 4.
Forest plot shows subset analysis of preferred sequence. Summary estimate (*diamond*)
indicates that overall preference for 2D fast spin-echo (FSE) or 3D FSE sequence is also
almost equally distributed, with nonsignificant tendency in favor of 2D FSE sequence.
Dashed line denotes summary measure.

TABLE 1

Intraobserver Agreement of Preferred T2-Weighted MR Sequence Among Duplicate Slides, by Individual Radiologist

Radiologist	No. (%) of Agreements	*p*
Reader 2	15/15 (100)	0.008
Reader 1	14/15 (93)	0.02
Reader 4	13/15 (87)	0.03
Reader 6	12/15 (80)	0.06
Reader 3	11/15 (73)	0.14
Reader 5	9/15 (60)	0.40

TABLE 2

Preferred Sequence in the Review of 100 Paired T2-Weighted MR Images, by Individual Radiologist

Radiologist	Technique	
	2D FSE	3D FSE
Reader 2	89	11
Reader 1	87	13
Reader 6	67	33
Reader 4	30	70
Reader 3	23	77
Reader 5	20	80

Note—Data are both no. and percentages. FSE = fast spin-echo.

TABLE 3

Results of the Multivariate Logistic Regressions

Parameter	Odds Ratio	95% CI	*p*
Treatment			
EBRT	1.05	0.46–2.40	0.91
Brachytherapy[a]	0.73	0.42–1.25	0.25
ADT	0.63	0.20–2.03	0.44
Cryoablation	1.24	0.39–4.0	0.72
Radiologist			
Reader 2	0.91	0.50–1.66	0.76
Reader 3	0.87	0.47–1.59	0.64
Reader 4	0.79	0.43–1.44	0.44
Reader 5	0.91	0.50–1.66	0.76
Reader 6	1.05	0.57–1.90	0.88
Reader experience (y)	1.23	0.79–1.90	0.35

Note—Model includes all radiologists. Positive outcome is the option for 3D fast spin echo. EBRT = external beam radiation therapy, ADT = androgen deprivation therapy.

[a] Permanent prostatic implant.

TABLE 4

Comparison of Mean Scores for Confidence in Tumor Identification on 2D and 3D Fast Spin-Echo (FSE) MR Images, by Individual Radiologist and for All Readers

Technique	Radiologist(s)						All
	Reader 1	Reader 2	Reader 3	Reader 4	Reader 5	Reader 6	
2D FSE	3.14 (1.35)	4.14 (0.95)	3.64 (1.22)	3.71 (1.27)	4.00 (0.68)	3.29 (1.38)	3.63 (1.07)
3D FSE	3.14 (1.41)	3.86 (0.77)	3.64 (1.01)	3.71 (1.07)	4.07 (0.73)	3.36 (1.22)	3.65 (1.19)
p	1.00	0.16	1.00	1.00	0.78	0.87	0.67

Note—Except where otherwise indicated, data are mean scores with SDs given in parentheses.

TABLE 5

Comparison of Mean Scores for Anatomic Delineation and Image Quality, for All Readers

			Parameter			
Technique	Zonal Anatomy	Capsule Delineation	Tumor Conspicuity	Image Sharpness	Image Distortion	Motion Artifact	Other Artifacts
2D FSE	2.57 (0.57)	2.25 (0.51)	2.44 (0.65)	2.67 (0.47)	2.71 (0.45)	2.71 (0.45)	2.21 (0.49)
3D FSE	2.46 (0.57)	2.34 (0.53)	2.45 (0.65)	2.21 (0.49)	2.65 (0.48)	2.76 (0.43)	2.46 (0.53)
p	0.19	0.14	0.89	< 0.001	0.41	0.48	0.002

Note—Except where otherwise indicated, data are mean scores with SDs given in parentheses. FSE = fast spin-echo.